Surface self-diffusivity of TiO_2 under high-pressure gas

Makoto Nanko* and Kozo Ishizaki
Nagaoka Gijutsu-Kagaku Daigaku (Nagaoka University of Technology), School of Mechanical Engineering, Nagaoka, Niigata 940-21, Japan
(Received 22 April 1997)

The surface diffusion coefficient of TiO_2 under a high-pressure gas of 100 MPa was estimated by using simulation of a sintering model consisting of surface and volume diffusion. The value of the volume diffusion coefficient of TiO_2 estimated using the present simulation is similar to the value of the diffusion coefficient of oxygen in TiO_2. The surface diffusivity was considered independently of the inert gas atmosphere. The present work, however, shows that the value of the surface diffusion coefficient of TiO_2 under a high-pressure argon gas of 100 MPa is about 30 times higher than that under 1 atm. [S0163-1829(97)07631-5]

I. INTRODUCTION

Hot isostatic processing (HIPing), i.e., sintering powder compacts under high-pressure gas, allows one to produce porous materials with higher open porosity than conventionally sintered bodies at the same temperatures.[1,2] HIPed porous materials possess a higher apparent Young's modulus[3] and higher fluid permeability[4] than conventionally sintered ones with the same density. The properties of HIPed porous materials result from a larger neck growth with less densification than porous materials sintered conventionally. This phenomenon under HIPing implies that high-pressure gases enhance surface diffusion, which prevents densification due to the reduction of the driving force of densification by sintering, i.e., the reduction of the surface area. Materials sintered partially under high-pressure gases have lower surface areas than ones sintered under low-pressure gases.[5]

Previously, we reported that HIPed porous copper has more grown steps on the surface than conventionally sintered one.[6] With increasing HIPing pressure, the formed steps become larger. On the other hand, the HIPing for sintering abrasive grains with a glassy bonding agent made for a smoother pore surface than conventional sintering. In this material, the surface is coated by a glassy bonding agent, which is an amorphous material.[6] The differences between pore surface morphologies of the HIPed materials are caused by the differences of the final equilibrium surface morphologies of crystalline or amorphous materials. Due to the enhancement of surface diffusion, surface morphology becomes an equilibrium state faster under high-pressure gas. In crystalline solids, an equilibrium of the surface morphology is achieved by the formation and growth of steps which are comprised of crystal facets with the lowest specific surface Gibbs energy. In amorphous materials, a surface becomes smoother for a decreasing surface area, i.e., a lower total surface energy, because amorphous materials have no crystalline facets. Thus the enhancement of surface diffusion by high-pressure gas is revealed from the observation of surface morphology.

A simulation of sintering with surface diffusion is useful in order to confirm the increased surface diffusivity by high-pressure gases. A surface diffusion coefficient under high-pressure gases can also be estimated by using the simulation of sintering. A kinetic model of sintering that explains the changes in density and surface area is established to investigate the obtained sintering behavior under high-pressure gases. Such a model has never been reported, to the best knowledge of the authors.

In the present work, the effects of 100 MPa of highly pressurized argon on surface diffusivity are investigated by sintering with a calculation using a sintering model based on volume and surface diffusion. Changes in the densities and surface areas of a sintered body having random packing with spherical particles are calculated. The values of the surface and volume diffusion coefficients of TiO_2 are estimated by using the sintering results of TiO_2.

II. THEORY

Figures 1(a), 1(b), and 1(c) show schematic illustrations of a neck between two particles. Volume diffusion causes neck growth with interpenetration of particles, Y in Fig. 1(a), i.e., approaching the center of the particle of the other one. In other words, densification occurs by volume diffusion.[7,8] On the other hand, surface diffusion causes neck growth with no densification.[7,8]

The following equations derived by using the sintering model of Kuczynski[9] are based in order to estimate the neck growth rate controlled by volume diffusion, dX_v/dt, and that by surface diffusion, dX_s/dt:

$$\frac{dX_v}{dt}=\frac{8a^2\gamma\delta^3 D_v}{C^2X^4kT}, \tag{1}$$

$$\frac{dX_s}{dt}=\frac{32a^3\gamma\delta^4 D_s}{C^3X^6kT}, \tag{2}$$

where γ, δ^3, D, k and T are the surface tension, atomic volume, diffusion coefficient, Boltzmann constant, and absolute temperature, respectively. The subscripts S and V refer to the surface and volume, respectively. Here we introduce a geometrical constant C, which relates radii of the neck X, particle a, and the neck surface ρ, as follows:

$$\rho=\frac{CX^2}{4a}. \tag{3}$$

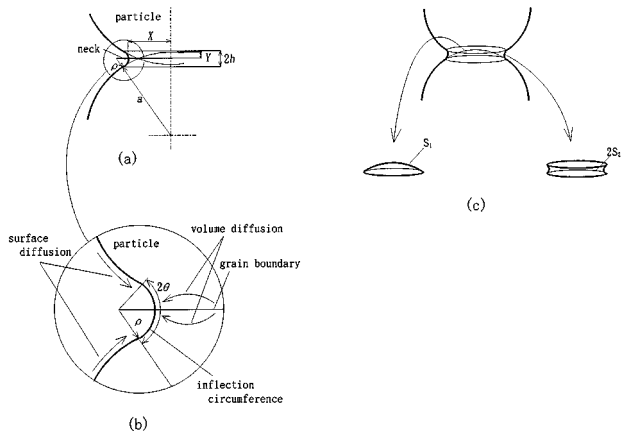

FIG. 1. Schematic illustrations of the neck part between two particles: (a) a cross-sectional drawing of two connected particles during sintering. (b) Details of the neck part and mass-transport paths of the volume and surface diffusion. (c) A particle surface disappeared by sintering (surface area S_1) and a neck surface created by sintering (surface area S_2). In these illustration, X, a, and ρ are the radii of the neck, the particle, and the neck surface. The interpretation depth is represented by Y. The distance between the two inflection circumference planes is defined as $2h$, and the angle 2θ. Surface S_1 disappears and S_2 generates through sintering.

The value of C is equal to 1 in the case of sintering dominated by mass transports with densification, and is equal to 2 in the case of sintering dominated by mass transports without densification.[7] In this simulation, the value of C is assumed to be equal to 1.5, because of the contribution of both surface and volume diffusion to the sintering.

The total neck growth rate dX_{tot}/dt during sintering is assumed to be the sum of the neck growth rates of volume and surface diffusion, as follows:

$$\frac{dX_{\mathrm{tot}}}{dt}=\frac{dX_v}{dt}+\frac{dX_s}{dt}. \tag{4}$$

Particles adhere and form small necks during compaction of green bodies. Accordingly, the neck radius X can be represented by

$$X=X_{t=0}+\sum \frac{dX_{\mathrm{tot}}}{dt}\Delta t. \tag{5}$$

The volume diffusion mechanism causes interpenetration of particles, which results in densification during sintering. The following relationship between the interpenetration of a particle and the neck growth of volume diffusion is derived from the volume balance

$$A_x dY=A_\rho dX_v, \tag{6}$$

where A_ρ and A_X indicate the neck surface area and neck cross-sectional area and are expressed by πX^2 and $2\pi X \times \pi\rho$, respectively. From Eq. (6), the interpenetration rate dY/dt can be represented as the following equation by using the neck growth resulting from volume diffusion:

$$\frac{dY}{dt}=\frac{A_\rho}{A_X}\frac{dX_v}{dt}. \tag{7}$$

Therefore the interpenetration depth Y can be obtained by integrating Eq. (7).

When particle packing is homogeneous, linear shrinkage $\Delta l/l_0$ can be expressed by

$$\frac{\Delta l}{l_0}=\frac{Y}{a}. \tag{8}$$

Volume shrinkage $\Delta V/V_0$ is equal to $3(\Delta l/l_0)$ if $\Delta l/l_0$ is sufficiently small. Accordingly, the density change $\Delta d/d_0$ is derived form $\Delta V/V_0$, and is represented as

$$\frac{\Delta d}{d_0}=\frac{3Y}{a-3Y}. \tag{9}$$

Now let us calculate the change in surface area. As shown in Fig. 1(c), a portion of the particle surface S_1 disappears, and the neck surface S_1 disappears, and the neck surface S_2 is created by sintering. The following equations allow us to calculate S_1 and S_2 geometrically:

$$S_1=2\pi a(h+Y)=2\pi a\left(\frac{CX^2(a-Y)}{4a^2+CX^2}+Y\right), \tag{10}$$

$$S_2=2\pi X\rho\theta=\frac{C\pi X^4}{2a}\sin^{-1}\left(\frac{4a(a-Y)}{C(4a^2+X^2)}\right), \tag{11}$$

where the distance between the two inflection circumference planes is defined as $2h$, and the angle 2θ as seen in Figs. 1(a) and 1(b). The reduction of the surface area during sintering, $\Delta s_s/s_{s0}$, can be expressed as follows:

$$\frac{\Delta s_s}{s_{s0}}=\frac{N_c(S_1-S_2)}{4\pi a^2}, \tag{12}$$

where s_{s0} is the initial value of the total surface area, and N_c is the mean coordination number of particles. Thus the dependence of the density and the surface area on the sintering time can be estimated by using Eqs. (9) and (12).

The value of D_v and D_s of TiO_2 during sintering are estimated by this model. In the present estimation, the values of γ and δ^3 are assumed to be constant in both conventional sintering and HIPing. It is assumed that the influences of highly pressurized argon under 100 MPa on surface tension and atomic volume are negligibly small, because the compressibility of TiO_2 is small enough and argon is chemically inert to surface of the oxide.

German and Munir reported a kinetic model for the reduction in surface area during sintering.[10] Their sintering model is based on the Kuczynski's neck growth mechanism with one dominant diffusion mechanism. According to them, their model can be applied until the neighboring necks contact each other when Δs_s becomes around half of s_{s0}.[10]

The Kuczynski model can be applied to estimate neck growth of the initial stage of sintering,[7] with X up to $0.3a$. The present model, however, was applied to $X=0.5a$, be-

TABLE I. Specification of the raw TiO_2 powder.

Supplier and grade	Ishihara Sangyo Co., EL-CR
Major phase	rutile
Purity	99.7%
Elementary particle size	0.3 μm
Specific surface area	7 m^2/g

cause the simulation results on d and s_s as a function of t up to $X=0.5a$, agreed well with the experimental results.

III. EXPERIMENTS

A rutile-type TiO_2 powder is used (see Table I). Figure 2 shows the scanning-electron-microscope photograph of the raw TiO_2 powder. This powder is roundish in particle shape, and homogeneous in particle size distribution. This powder was uniaxially pressed under 7 MPa for 60 s to form a pellet of 20-mm diameter and about 3.5-mm thickness. The density reached to 0.50 of the theoretical density. The uniaxially pressed compacts were cold isostatically pressed (CIPed) under 20 MPa for 60 s. The density of the CIPed bodies increased to 0.52 of the theoretical density. The density of the CIPed body was measured by the toluene displacement method.

The CIPed TiO_2 compacts were HIPed at 800 °C for periods ranging from 1 to 10 h (3.6 to 36 ks) under 100 MPa of total gas pressure with 0.1 MPa of oxygen partial pressure by using a gas mixture of Ar and 0.1 vol % O_2. The conventionally sintered bodies were obtained by sintering the CIPed samples at 800 and at 850 °C for periods ranging from 1 to 10 h (3.6 to 36 ks) under continuous oxygen flow of 1 atm. Thus, in order to discuss effects of highly pressurized argon under 100 MPa without effects of oxygen partial pressure, the oxygen partial pressure is about 0.1 MPa in both sintering cases. The heating rate was 400 K/h for both cases. Cooling processes in both conventional sintering and HIPing are carried out rapidly by gas flow and adiabatic expansion from the sintering temperature to about 600 °C in order to reduce

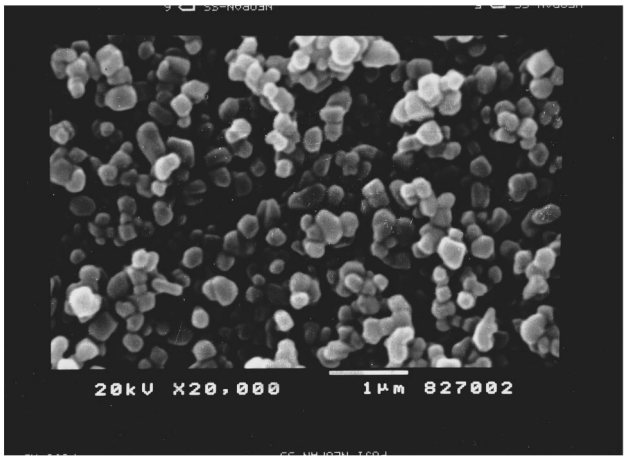

FIG. 2. SEM photograph of the starting TiO_2 powder. This powder is homogeneous and roundish in particle shape. The particle diameter is about 0.3 μm.

influences of the cooling period on the sintering.

The density and porosity of the sintered materials were measured by the water displacement method. The specific surface area of the samples was measured by the one-point Brunaver-Emmett-Teller method.

For the calculation of the changes of density and surface area, the following values were used. The initial particle size of TiO_2 particles was considered as 0.3 μm. A powder compact in the present simulation was assumed to have a random packing of particles and to have 0.52 of the theoretical density. The specific surface area of the initial powder compact is 4.62 m^2/g from the calculation using the particle size. The values of the density fraction and the surface area were in good agreement with the measured values of the real powder compacts (0.52 and 4.8 m^2/g). According to a computer simulation on isostatic compaction,[11] a powder compact with d of 0.52 has an N_c of about 6. Jernot, Coster, and Chermant summarized the relationship between N_c and d on the powder compact.[12] According to their work, the value of d of 0.52 in the present study corresponds to the value of about 6 for N_c. The value of N_c was assumed to be constant, i.e., there was no rearrangement of particle packing during sintering. For this calculation of TiO_2, the surface tension γ and atomic volume δ^3 are assumed to be 1 N/m and 1.6×10^{-29} m^3, respectively.[13] The thickness of the surface layer is assumed to be δ.

IV. RESULTS

Figure 3 shows d and s_s as functions of t on the sintering TiO_2 under different sintering conditions. In Fig. 3(a), the data of the conventionally sintered sample at 800 and at 850 °C, and (b) the data of the HIPed samples at 850 °C, are plotted. The data of the conventionally sintered samples at 850 °C are also included in Fig. 3(b).

The lines plotted in Fig. 3(a) are the results of the present calculation, where $X_{t=0}$ is assumed to be 5 nm, and is insensitive to the results. The calculated results using the values of $D_v=3.5\times 10^{-20}$ m^2/s and $D_s=6.5\times 10^{-18}$ m^2/s agree well with the experimental ones of conventional sintering at 800 °C up to 20 ks. The values of 1.5×10^{-19} m^2/s of D_v and 8.0×10^{-18} m^2/s of D_s give results close to the sintering behavior at 850 °C up to 7.2 ks. These deviations of the calculation may be due to the approximation of ρ by X and a at the basis of the model of Kuczynski. This model is for the initial stage on sintering up to $X=0.3a$. In this calculation, the values of X/a after 36 ks at 800 °C and after 7.5 ks at 850 °C are 0.47 and 0.46, respectively. By using the established model in the present work, the sintering behavior can be estimated up to $X=0.5a$. The HIPing data agree with the calculated results of $D_v=1.5\times 10^{-19}$ m^2/s and $D_s=2.2\times 10^{-16}$ m^2/s. The value of D_v for HIPing, 1.5×10^{-18} m^2/s, is similar to that of the conventional sintering at 850 °C. Table II shows the results of D_v and D_s for different temperatures and gas pressures.

V. DISCUSSION

Evaporation-condensation is also a sintering mechanism without densification.[7,8] In this experiment, the sintering temperatures are sufficiently lower than the melting point,

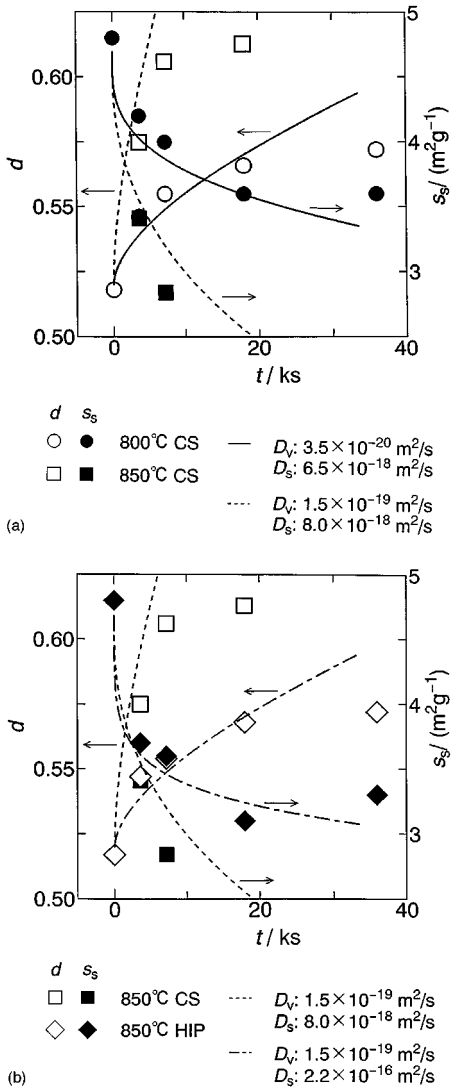

FIG. 3. (a) d and s_s as a function of t for sintered TiO_2 under 1 atm of oxygen at 800 and 850 °C. The solid line represents the calculated result of $D_\nu = 3.5\times10^{-20}$ m^2/s and $D_s = 6.5\times10^{-18}$ m^2/s. The broken line expresses the result of $D_\nu = 1.5\times10^{-19}$ m^2/s and $D_s = 8\times10^{-18}$ m^2/s. The circles and squares represent the data for sintering at 800 and 850 °C, respectively. The solid and open symbols designate the data for d and s_s, respectively. The calculated results of $D_\nu = 3.5\times10^{-20}$ m^2/s and $D_s = 5.4\times10^{-18}$ m^2/s agree well with the data for sintering at 800 °C. The result of $D_\nu = 1.5\times10^{-19}$ m^2/s and $D_s = 8.0\times10^{-18}$ m^2/s are in agreement with those at 850 °C. (b) d and s_s as a function of t with conventional sintering of TiO_2 at 850 °C. The broken line expresses the result of $D_\nu = 1.5\times10^{-19}$ m^2/s and $D_s = 8.0\times10^{-16}$ m^2/s. The one-dot-chain line represents the calculated result of $D_\nu = 1.5\times10^{-19}$ m^2/s, which is the same value of the HIPing, and $D_s = 2.2\times10^{-16}$ m^2/s. The squares represent the data of HIPed TiO_2. The value of D_s increases 30 times by high-pressure gases of 100 MPa.

2113 K. The equilibrium vapor pressure of TiO_2 is very low ($\approx10^{-18}$ Pa) at 850 °C, according to the thermodynamic data.[14] The flux of the mass transport by TiO_2 vapor is negligibly smaller than that of the surface diffusion. Furthermore, evaporation of TiO_2 was prevented by high-pressure gas during HIPing. Therefore the influences of the evaporation-condensation mechanism is negligible in the present sintering experiment.

TABLE II. Surface and volume diffusion coefficients of TiO_2 at different temperatures under gas pressures. The oxygen partial pressure is about 0.1 MPa for all cases. T: sintering temperature; P_{tot}: sintering pressure.

T/°C	800	850	850
P_{tot}/MPa	0.1	0.1	100
D_ν/(m^2/s)	3.5×10^{-20}	1.5×10^{-19}	1.5×10^{-19}
D_s/(m^2/s)	6.5×10^{-18}	8.0×10^{-18}	2.2×10^{-16}

The values of D_ν of conventional sintering, 3.5×10^{-20} m^2/s at 800 °C and 1.5×10^{-19} m^2/s at 850 °C. These values of D_ν are respectively close to the values of O ion in TiO_2, 4.2×10^{-20} m^2/s at 800 °C and 1.7×10^{-19} m^2/s at 850 °C, extrapolated by using the data reported by Derry, Lees, and Calvert.[15] This means that the sintering of TiO_2 is dominated by diffusion of O ion in TiO_2. Generally, sintering of compounds is governed by the diffusion of ions with the slowest diffusion coefficients.[16] In the case of TiO_2, the O ion has a smaller diffusion coefficient than the Ti ion, because interstitial Ti^{3+} is the dominant defect in TiO_2.[16] Accordingly, the calculated value of D_ν for conventionally sintered TiO_2 is inevitably similar to the volume diffusion coefficient of the O ion of TiO_2. Therefore the present simulation is a valid method to estimate the sintering of TiO_2.

The value of D_s at 850 °C under 100 MPa of high-pressure gas is about 30 times higher than that under 1 atm, in spite of the same value of D_ν. This means that high-pressure argon of 100 MPa enhances a surface diffusivity of TiO_2.

Enhancement of surface diffusion by high-pressure gases may be due to an increase of a number of gas atoms that collide with surface atoms per unit time and area. Collusion of gas atoms or molecules activates surface atoms to diffuse easily. High-pressure gas has more gas atoms or molecules per unit volume than gas under ordinary pressure. For example, a high-pressure gas of 100 MPa has 1000 times more gas atoms or molecules per unit volume than one of 0.1 MPa, assuming an ideal gas. Accordingly, a high-pressure gas under 100 MPa has 1000 times more collisions of gas atoms and molecules with surface atoms than one under 0.1 MPa. This large number of collision frequencies of gas atoms or molecules with surface atoms enhances the vibration of surface atoms, and therefore forces them to diffuse on the surface.

VI. CONCLUSIONS

Effects of 100 MPa of highly pressurized argon on sintering behavior were investigated by using a simulation model that combines the effects of volume and surface diffusion. The values of the surface and volume diffusion coefficients of TiO_2 under a high-pressure gas of 100 MPa were obtained by this model using the results of sintering of TiO_2. The value of D_s under high-pressure argon under 100 MPa (2.2×10^{-16} m^2/s at 850 °C) is about 30 times higher than that of

oxygen under 1 atm (8.0×10^{-18} m^2/s at 850 °C). High-pressure gas enhances surface diffusion. The obtained value of the volume diffusion coefficient of TiO_2 is in good agreement with the value of the volume diffusion coefficient of O in TiO_2, i.e., 3.5×10^{-20} m^2/s at 800 °C and 1.5×10^{-19} m^2/s at 850 °C.[17]

ACKNOWLEDGMENTS

The authors would like to thank Ishihara Sangyo Co. for supplying the TiO_2 powder used in the present study. This research was partially carried out under a financial support of the Japan Society for the Promotion of Science. The authors wish to express their gratitude for their support.

*Present Address: Tokyo Institute of Technology, Department of Metallurgical Engineering, Meguro, Tokyo 152, Japan.

[1] K. Ishizaki, A. Takata, and S. Okada, J. Ceram. Soc. Jpn. **98**, 533 (1990).

[2] K. Ishizaki, S. Okada, T. Fujikawa, and A. Takata, Germany Patent No. P 40 91 346.5 (May 1996): US Patent No. 5,126,103 (June 1992); Japan Patent Pending, Hei 1-205421 (1989).

[3] A. Takata, K. Ishizaki, Y. Kondo, and T. Shioura, in *Pressure Effects on Materials Processing and Design*, edited by K. Ishizaki, E. Hodge, and M. Concannon, MRS Symposia Proceedings No. 251 (Materials Research Society, Pittsburgh, 1992), pp. 133–138.

[4] M. Nanko, K. Ishizaki, and T. Fujikawa, J. Am. Ceram. Soc. **77**, 2437 (1994).

[5] M. Nanko, K. Ishizaki and T. Fujikawa, J. Am. Ceram. Soc. **78**, 1695 (1995).

[6] M. Nanko, K. Ishizaki and A. Takata, in *Ceramic Transactions, Vol. 31, Porous Materials*, edited by K. Ishizaki, L. Sheppard, S. Okada, M. Hamasaki, and B. Huybrechts (American Ceramic Society, Westerville, OH, 1993), pp. 117–126.

[7] K. Hamano and S. Kimura, *Fain Seramikkusu Kiso Kagaku* (Asakura Syoin, Tokyo, 1990), pp. 67–72.

[8] W. D. Kingery and M. Berg, J. Appl. Phys. **26**, 1205 (1955).

[9] G. C. Kuczynski, Trans. AIME **185**, 169 (1949).

[10] R. M. German and Z. A. Munir, J. Am. Ceram. Soc. **59**, 379 (1976).

[11] Y. Konakawa and K. Ishizaki, Powder Technol. **63**, 241 (1990).

[12] J. P. Jernot, M. Coster, and J. L. Chermant, Powder Technol. **30**, 21 (1981).

[13] Y. Moriyoshi and W. Komatsu, Yogyo-Kyokai-Shi **81**, 28 (1973).

[14] O. Knacke, O. Kubaschewski, and K. Hesselmann, *Thermochemical Properties of Inorganic Substances*, 2nd ed. (Springer-Verlag, Berlin, 1991), pp. 2097–2099.

[15] D. J. Derry, D. G. Lees, and J. M. Calvert, J. Phys. Chem. Solids **42**, 57 (1981).

[16] K. Fueki and S. Yamauchi, in *Kagaku-Soron: Reactivity of Solids*, edited by The Chemical Society of Japan (Gakkai-Syuppan Senta, Tokyo, 1975), Chap 3, p. 41.

[17] K. Hoshino, N. L. Peterson, and C. L. Wiley, J. Phys. Chem. Solids **46**, 1397 (1981).